Karlsruhe Institute of Technology

# The parallel finite element system M++

Christian Wieners

Institut für Angewandte und Numerische Mathematik

# Meshes, multigrid and more: M++

We summarize the general concepts of M++ documented in

The parallel finite element system M++ with integrated multilevel preconditioning and multilevel Monte Carlo methods
N. Baumgarten and C. Wieners
Computers & Mathematics with Applications 81, pp. 391-406 (2021)
https://doi.org/10.1016/j.camwa.2020.03.004
preprint http://www.math.kit.edu/user/ wieners/BaumgartenWieners2019.pdf

More details and the link to the code are given on

https://www.math.kit.edu/ianm3/page/mplusplus

Installing and compiling details on

https://gitlab.kit.edu/kit/mpp/mpp

and in README.md

# A tutorial for scientific computing

Karlsruhe Institute of Technology

Complemented to a lecture on scientific computing we introduce a tutorial, where main features of finite element discretizations for elliptic, hyperbolic, and parabolic equations are evaluated by a sample application in porous media.

```
git clone -recurse-submodules https://gitlab.kit.edu/kit/mpp/mpp
cd mpp
mkdir build
cd build
cmake ..  -DBUILD_TUTORIAL=ON -DUSE_SPACETIME=ON
make -j
mpirun -n 8 M++ TUT_elliptic Problem=LaplaceSquare500 level=5
paraview data/vtu/u.vtu                                    select in 'Solid Color' value0
```

Configuration in `mpp/conf/TUT_elliptic.conf`
Problem definition in `mpp/src/lib6_app/problems/EllipticProblems.cpp`
Results in `mpp/build/log/logfile.log`

```
mpirun -n 8 M++ TUT_pollution
paraview data/vtu/PollutionSquare500...vtu
```

```
mpirun -n 8 M++ TUT_reaction
paraview data/vtu/C...vtu
```

# Cells, faces, edges, vertices

The main concept of the parallel data structure in M++ is the unique identification of geometric objects by their midpoints represented in space $x \in \mathbb{R}^d$ with $d \in \{1, 2, 3\}$ or in space-time $(t, x) \in \mathbb{R}^{1+d}$ (requires `cmake .. -DUSE_SPACETIME=ON`)

**Mesh representation**. A mesh $\mathcal{M} = (\mathcal{V}, \mathcal{K}, \mathcal{F}, \mathcal{E})$ is determined by a set of vertices $\mathcal{V}$, cells $\mathcal{K}$, faces $\mathcal{F}$, and edges $\mathcal{E}$. A cell $K \in \mathcal{K}$ is represented by its vertices $\mathcal{V}_K \subset \mathcal{V}$, an edge $E \in \mathcal{E}$ by $\mathcal{V}_E \subset \mathcal{V}$, a face $F \in \mathcal{F}$ by $\mathcal{V}_F \subset \mathcal{V}$. This defines

$$\mathcal{E}_K = \left\{ E \in \mathcal{E} \colon \mathcal{V}_E \subset \mathcal{V}_K \right\}, \qquad \mathcal{F}_K = \left\{ F \in \mathcal{F} \colon \mathcal{V}_F \subset \mathcal{V}_K \right\}.$$

A mesh is admissible if

$$\operatorname{conv}(\mathcal{V}_K \cap \mathcal{V}_{K'}) = \operatorname{conv} \mathcal{V}_K \cap \operatorname{conv} \mathcal{V}_{K'} \quad \text{for} \quad K, K' \in \mathcal{K}.$$

Every cell $K \in \mathcal{K}$ is associated with a reference cell $\hat{K}$, i.e., a reference interval in $d = 1$, a reference triangle or quadrilateral in $d = 2$, a reference tetrahedron, pyramid, prism, or hexahedron in $d = 3$ or a reference elements in space-time built as tensor product of an interval in time and a reference element in space.
All reference cells $\hat{K}$ are determined by vertices $\mathcal{V}_{\hat{K}}$, edges $\mathcal{E}_{\hat{K}}$, and faces $\mathcal{F}_{\hat{K}}$ represented by a vector of vertices $\hat{z}_1, \ldots, \hat{z}_{|\mathcal{V}_{\hat{K}}|}$ in $\mathbb{R}^d$ or $\mathbb{R}^{d+1}$, edge numbers $(e_{1k}, e_{2k})_{k=1,\ldots,|\mathcal{E}_{\hat{K}}|}$, and face numbers $(f_{jk})_{j=1,\ldots,|\mathcal{V}_{\hat{F}_k}|, k=1,\ldots,|\mathcal{F}_{\hat{K}}|}$.

`mpp/src/lib2_mesh/mesh/Mesh.hpp`

# Unit cube

```
HEADER:
Checked=true
WithData=false
Cellformat=Vtu
POINTS:
0 0 0
1 0 0
1 1 0
0 1 0
0 0 1
1 0 1
1 1 1
0 1 1
CELLS:
12 0 0 1 2 3 4 5 6 7
FACES:
```

mpp/conf/geo/UnitCube.geo

# Unit cube

```
POINTS
0.00 0.00 0.00
1.00 0.00 0.00
1.00 1.00 0.00
0.00 1.00 0.00
0.00 0.00 1.00
1.00 0.00 1.00
1.00 1.00 1.00
0.00 1.00 1.00
0.500000 0.500000 0.000000
0.500000 0.000000 0.500000
1.000000 0.500000 0.500000
0.500000 1.000000 0.500000
0.000000 0.500000 0.500000
0.500000 0.500000 1.000000
0.500000 0.500000 0.500000
CELLS
4 0 14 8 0 1
4 0 14 8 1 2
4 0 14 8 2 3
4 0 14 8 3 0
4 0 14 9 0 1
4 0 14 9 1 5
4 0 14 9 5 4
4 0 14 9 4 0
4 0 14 10 1 2
4 0 14 10 2 6
4 0 14 10 6 5
4 0 14 10 5 1
4 0 14 11 2 3
4 0 14 11 3 7
4 0 14 11 7 6
4 0 14 11 6 2
4 0 14 12 3 0
4 0 14 12 0 4
4 0 14 12 4 7
4 0 14 12 7 3
4 0 14 13 4 5
4 0 14 13 5 6
4 0 14 13 6 7
4 0 14 13 7 4
FACES
3 0 0 1 8
3 0 1 2 8
3 0 2 3 8
3 0 3 0 8
3 0 0 1 9
3 0 1 5 9
3 0 5 4 9
3 0 4 0 9
3 0 1 2 10
3 0 2 6 10
3 0 6 5 10
3 0 5 1 10
3 0 2 3 11
3 0 3 7 11
3 0 7 6 11
3 0 6 2 11
3 0 0 3 12
3 0 3 7 12
3 0 7 4 12
3 0 4 0 12
3 0 4 5 13
3 0 5 6 13
3 0 6 7 13
3 0 7 4 13
```

# Parallel mesh distribution

The construction of the initial mesh is a sequential process. We assume that the vertices $\mathcal{V}_K$ are given by a vector $(z_1, \dots, z_{|\mathcal{V}_K|})$. Then the elements $K \in \mathcal{K}$ are determined by an identification number to the associated reference element $\hat{K}$ and the vector of vertex numbers $(n_k)_{k=1,\dots,|\mathcal{V}_K|}$, such that

$$\begin{aligned} \mathcal{V}_K &= \{z_{n_k} : k = 1, \dots, |\mathcal{V}_K|\}, \\ \mathcal{V}_{E_k} &= \{z_{n_{e_{1k}}}, z_{n_{e_{2k}}}\}, && k = 1, \dots, |\mathcal{E}_{\hat{K}}|, \\ \mathcal{V}_{F_k} &= \{z_{n_{f_{jk}}} : j = 1, \dots, |\mathcal{V}_{\hat{F}_k}|\}, && k = 1, \dots, |\mathcal{F}_{\hat{K}}|. \end{aligned}$$

We assume that the numbering defines an injective orientation preserving mapping (which is affine linear for intervals, triangles, and tetrahedra)

$$\varphi_K : \operatorname{conv} \mathcal{V}_{\hat{K}} \longrightarrow \operatorname{conv} \mathcal{V}_K \qquad \text{with} \qquad \varphi_K(\hat{z}_k) = z_{n_k}, \ k = 1, \dots, |\mathcal{V}_K|. \tag{1}$$

Cells, edges, and faces are represented by its midpoints

$$z_K = \frac{1}{|\mathcal{V}_K|} \sum_{z \in \mathcal{V}_K} z, \qquad z_E = \frac{1}{|\mathcal{V}_E|} \sum_{z \in \mathcal{V}_E} z \qquad z_F = \frac{1}{|\mathcal{V}_F|} \sum_{z \in \mathcal{V}_F} z,$$

and we define the set $\mathcal{Z} = \mathcal{V} \cup \mathcal{Z}_\mathcal{K} \cup \mathcal{Z}_\mathcal{E} \cup \mathcal{Z}_\mathcal{F}$ with

$$\mathcal{Z}_\mathcal{K} = \{z_K : K \in \mathcal{K}\}, \qquad \mathcal{Z}_\mathcal{E} = \{z_E : E \in \mathcal{E}\}, \qquad \mathcal{Z}_\mathcal{F} = \{z_F : F \in \mathcal{F}\}.$$

# Parallel mesh distribution

Then, we provide mappings

$$\mathcal{Z}_{\mathcal{K}} \longrightarrow \mathcal{V} \times \cdots \times \mathcal{V}\,, \qquad z_K \longmapsto \left(z_{K,1}, \ldots, z_{K,|\mathcal{V}_K|}\right), \tag{2a}$$

$$\mathcal{Z}_{\mathcal{E}} \longrightarrow \mathcal{V} \times \mathcal{V}\,, \qquad z_E \longmapsto \left(z_{E,1}, z_{E,2}\right), \tag{2b}$$

$$\mathcal{Z}_{\mathcal{F}} \longrightarrow \mathcal{V} \times \mathcal{V}\,, \qquad z_F \longmapsto \left(z_K, z_{K'}\right), \tag{2c}$$

where $z_K$ maps to the vector of vertices of $K$, and $z_E$ maps to the pair of edge vertices.
For interior faces $F \in \mathcal{F}$, $z_F$ maps to the midpoints of the two cells $K$ and $K'$ with $\mathcal{F} = \mathcal{V}_K \cap \mathcal{V}_{K'}$, $K \neq K'$.
For boundary faces, $z_{K'} = \infty$ is set to a predefined exception point.
The full information on the mesh is contained in the data provided in the mappings (2).
They are realized by hash maps in order to provide $\mathcal{O}(1)$ access to the data.

`mpp/src/lib2_mesh/cells/Cell.hpp`

# Parallel mesh distribution

The mesh will be distributed to a set of processes $\mathcal{P} = \{1, \dots, P\}$.
The distribution is determined by a mapping

$$\mathrm{dest}\colon \mathcal{Z}_{\mathcal{K}} \longrightarrow \mathcal{P}\,,$$

which can be constructed by recursive coordinate bisection (RCB) using only the coordinates $\mathcal{Z}_{\mathcal{K}}$, or by recursive inertia bisection (RIB). We define process sets

$$\pi\colon \mathcal{Z} \longrightarrow 2^{\mathcal{P}}\,, \qquad \pi(z) = \begin{cases} \{\mathrm{dest}(z_K)\} & z = z_K \in \mathcal{Z}_{\mathcal{K}}\,, \\ \{\mathrm{dest}(z_K)\colon E \in \mathcal{E}_K\} & z = z_E \in \mathcal{Z}_{\mathcal{E}}\,, \\ \{\mathrm{dest}(z_K)\colon F \in \mathcal{F}_K\} & z = z_F \in \mathcal{Z}_{\mathcal{F}}\,, \\ \{\mathrm{dest}(z_K)\colon z \in \mathcal{V}_K\} & z \in \mathcal{V}\,. \end{cases}$$

This yields a non-overlapping distribution of the cells and overlapping distributions of the vertices, the edges, and the faces.
On process $p \in \mathcal{P}$, the local mesh $\mathcal{M}^p = (\mathcal{V}^p, \mathcal{K}^p, \mathcal{F}^p, \mathcal{E}^p)$ is given by

$$\begin{aligned} \mathcal{V}^p &= \{z \in \mathcal{V}\colon p \in \pi(z)\}\,, \\ \mathcal{K}^p &= \{K \in \mathcal{K}\colon p \in \pi(z_K)\}\,, \\ \mathcal{F}^p &= \{F \in \mathcal{F}\colon p \in \pi(z_F)\}\,, \\ \mathcal{E}^p &= \{E \in \mathcal{E}\colon p \in \pi(z_E)\}\,. \end{aligned}$$

For all geometric entities $z \in \mathcal{Z}$, $\mu(z) = \min \pi(z)$ defines the master process.

# Parallel mesh refinement

For every reference cell $\hat{K}$ a refinement rule

$$\mathcal{R}_{\hat{K}} = \{\hat{K}_1, \ldots, \hat{K}_{|\mathcal{R}_{\hat{K}}|}\}$$

is given by a vector of vertices for every refined cell $\hat{K}_j$. In case of uniform refinement, we have $|\mathcal{R}_{\hat{K}}| = 2^d$ for cells in space and $2^{1+d}$ for space-time cells. Starting with the parallel mesh $\mathcal{M}_0^p$ on level $l = 0$, this defines recursively $\mathcal{M}_l^p = (\mathcal{V}_l^p, \mathcal{K}_l^p, \mathcal{F}_l^p, \mathcal{E}_l^p)$ for $l = 1, \ldots, L$ by constructing locally

$$\mathcal{K}_l^p = \big\{ K_j : \text{cell with vertices } \mathcal{V}_{K_j} = \phi_K\big(\mathcal{V}_{\hat{K}_j}\big)\,,\ \hat{K}_j \in \mathcal{R}_{\hat{K}}\,,\ \hat{K} \text{ reference cell to } K \in \mathcal{K}_{l-1}^p \big\}\,.$$

For intervals, triangles, quadrilaterals and hexahedra one rule is sufficient for uniform refinement, in case of tetrahedra two rules are required in order to achieve a shape regular sequence of meshes.
Then the refinement rules for the cells are used for the refinement of faces and edges, and the corresponding process sets $\pi_l : \mathcal{Z}_l \longrightarrow 2^{\mathcal{P}}$ are constructed from $\pi_{l-1}$. In particular this defines $\pi_l(z_F)$ for faces on process interfaces, and the pair of neighboring cell midpoints $(z_K, z_{K'})$ to define (2c) is exchanged by local communication.

`mpp/src/lib2_mesh/cells/Cell.hpp`

# Parallel finite elements

A finite element discretization is determined by a triple $(\hat{K}, \hat{V}, \hat{V}')$ with reference cell $\hat{K}$, ansatz space $\hat{V} = \operatorname{span}\left\{\hat{\psi}_{\hat{z},j} : \hat{z} \in \hat{\mathcal{Z}},\ j = 1, \dots, N_{\hat{z}}\right\}$ and degrees of freedom $\hat{V}'$, i.e., functionals $\hat{\psi}'_{\hat{z},j}$ defining the discrete interpolation

$$\hat{v} = \sum \langle \hat{\psi}'_{\hat{z},j}, \hat{v} \rangle \hat{\psi}_{\hat{z},j} \in \hat{V}$$

in the reference cell. All basis functions $\hat{\psi}_{\hat{z},j}$ are associated to a point in $\hat{\mathcal{Z}}$, i.e, to the cell midpoint, an edge or face midpoint, or a vertex.
We assume that the corresponding degree of freedom $\hat{\psi}'_{\hat{z},j}$ can be evaluated by values in the cell, on the edge or face, or at the vertex.
For $K \in \mathcal{K}$, this is transformed to $(K, V_K, V'_K)$ by the mapping (1).
A cell $K \in \mathcal{K}$ is identified with an open subdomain $K \subset \mathbb{R}^d$ (or $K \subset \mathbb{R}^{1+d}$ in the space-time case) such that $\bar{K} = \operatorname{conv}(\mathcal{V}_K)$. This defines the open set $D_h = \bigcup_{K \in \mathcal{K}} K$ with skeleton $\partial D_h = \bigcup_{K \in \mathcal{K}} \partial K$. Let $\mathbb{P}_k(D_h) = \prod_K \mathbb{P}_k(D_h)$ be the discontinuous space of piecewise polynomials of degree $k$.
The local finite element spaces in $K$ are defined by its basis functions, i.e.,

$$V_K = \operatorname{span}\left\{\psi_{K,z,j} : z \in \mathcal{Z} \cap \bar{K},\ j = 1, \dots, N_z\right\},$$

which extends to the global finite element space in $D_h$ by

$$V_h = \operatorname{span}\left\{\psi_{z,j} : \psi_{z,j}|_K = \psi_{K,z,j} \in V_K \text{ for all } K \in \mathcal{K}\right\}.$$

Finite element functions are continuous or discontinuous on the skeleton $\partial D_h$.

# Parallel finite elements

Every local basis function $\psi_{K,z,j}$ is associated to a point $z \in \mathcal{Z} \cap \bar{K}$ with

- $z = z_K \in \mathcal{Z}_\mathcal{K}$, if $\operatorname{supp} \psi_{z,j} \subset \bar{K}$,
- $z = z_F \in \mathcal{Z}_\mathcal{F}$, if $\operatorname{supp} \psi_{z,j} \subset \bigcup_{F \in \mathcal{F}_K} \bar{K}$,
- $z = z_E \in \mathcal{Z}_\mathcal{E}$, if $\operatorname{supp} \psi_{z,j} \subset \bigcup_{E \in \mathcal{E}_K} \bar{K}$,
- $z \in \mathcal{V}$, if $\operatorname{supp} \psi_{z,j} \subset \bigcup_{z \in \mathcal{V}_K} \bar{K}$.

Within this framework, the following finite element spaces are realized.

**Conforming linear and quadratic Lagrange elements** $V_h^{\mathrm{c}} \subset \mathbb{P}_k(D_h) \cap \mathrm{C}^0(\bar{D})$.
We set $N_z = 1$ for $z \in \mathcal{V}$ and $k = 1$ for linear elements on intervals, triangles, and tetrahedra, bilinear elements on quadrilaterals, and trilinear elements on hexahedra; for the quadratic family we have $N_z = 1$ for $z \in \mathcal{V} \cup \mathcal{Z}_\mathcal{E}$ and $k = 2$.
The degrees of freedom are point evaluations.

**Raviart-Thomas elements** $W_h \subset \mathbb{P}_1(D_h; \mathbb{R}^d) \cap \mathrm{H}(\mathrm{div}, D)$.
We set $N_z = 1$ for $z \in \mathcal{Z}_\mathcal{F}$. The degrees of freedom are face averages of the normal flux on the face.
Note that this requires an orientation on the faces provided by (2c).

**Nedelec elements** $X_h \subset \mathbb{P}_1(D_h; \mathbb{R}^3) \cap \mathrm{H}(\mathrm{curl}, D)$.
We set $N_z = 1$ for $z \in \mathcal{Z}_\mathcal{E}$, and the degrees of freedom are integrals along the edges in the direction provided by (2b).

**Crouziex-Raviart elements** $V_h^{\mathrm{nc}} \subset \mathbb{P}_k(D_h)$.
We set $N_z = 1$ for $z \in \mathcal{Z}_\mathcal{F}$, and the degrees of freedom are face averages.

# Parallel finite elements

**Discontinuous Galerkin elements** $Q_{k,h} = \mathbb{P}_k(D_h)$.
We set $N_z = \dim(Q_K)$ for $z \in \mathcal{Z}_\mathcal{K}$ and the local spaces $Q_K = \mathbb{P}_k(K)$; the degrees of freedom are point evaluations in $\bar{K}$. This includes finite volume methods ($k = 0$) and adaptivity with local polynomial degrees $k_K$ depending on $K \in \mathcal{K}$.
**Enriched Galerkin elements** $V_h^{\mathrm{eG}} = V_h^{\mathrm{c}} + Q_{0,h} = \mathbb{P}_1(D_h) \cap \mathrm{C}^0(\bar{D}) + \mathbb{P}_0(D_h)$ .
Here, we use $N_z = 1$ for $z \in \mathcal{V} \cup \mathcal{Z}_\mathcal{Z}$ extending the conforming Lagrange elements by discontinuous finite volumes.
**Weakly conforming Galerkin elements** $V_h^{\mathrm{wc}}$.
We select a discrete discontinuous space $Q_{k,h} = \mathbb{P}_k(D_h; \mathbb{R}^d)$, and weak continuity is achieved by a Lagrange multiplier space $M_{k-1,h} = \prod_{F \in \mathcal{F}} \mathbb{P}_{k-1}(F; \mathbb{R}^d)$ defining

$$V_h^{\mathrm{wc}} = \left\{ v_h \in Q_{k,h} \colon \left( [v]_F, \lambda_h \right)_F = 0 \text{ for all } F \subset D \,, \lambda_h \in M_{k-1,h} \right\},$$

where $[v]_F = v|_{K'} - v|_K$ is the jump at interior faces. Hybrid skeleton reduction results into a positive definite Schur complement for the Lagrange multipliers.
**Discontinuous Petrov-Galerkin elements**.
Here, a general linear first-order system $Lu = f$ is formulated in weak form

$$(u, L^* w)_{D_h} + \langle \hat{u}, \mathrm{trace}^* w \rangle_{\partial D_h} = (f, w)_D$$

by introducing unknowns $\hat{u} = \mathrm{trace}\, u$ for the trace values on the skeleton.

`mpp/src/lib4_fem/elements/Element.hpp`

# Parallel linear algebra

A finite element function $v = \sum_{z,j} \underline{v}_{z,j} \psi_{z,j} \in V_h$ is determined by its coefficient vector $\underline{v} \in \underline{V} = \mathbb{R}^N$ with $N = \sum_{z,j} N_{z,j}$.
In parallel, this is represented by the embedding

$$\underline{e} \colon \underline{V} \longrightarrow \underline{V}^{\mathcal{P}} = \prod_{p \in \mathcal{P}} \underline{V}^p$$

into the overlapping space $\underline{V}^{\mathcal{P}}$ with $\underline{V}^p = \mathbb{R}^{N^p}$ and $N^p = \sum_{z \in \mathcal{Z}^p} \sum_j N_{z,j}$.
A parallel vector $\underline{v}^{\mathcal{P}} = (\underline{v}^p)_{p \in \mathcal{P}}$ is consistent, if $\underline{v}^{\mathcal{P}} \in \underline{e}(\underline{V})$, i.e.,

$$\underline{v}_z^p = \underline{v}_z^q \,, \qquad p, q \in \pi(z) \,,$$

A linear finite element solution $u_h \in V_h$ solves the linear equation

$$A_h u_h = b_h$$

with linear operator $A_h \colon V_h \longrightarrow V_h'$ and right-hand side $b_h \in V_h'$.
In parallel, the assembling is of the form

$$\langle A_h \psi_{z,j}, \phi_{y,k} \rangle = \sum_{p \in \mathcal{P}} a_h^p(\psi_{z,j}, \phi_{y,k}) \,, \qquad \langle b_h, \phi_{y,k} \rangle = \sum_{p \in \mathcal{P}} \ell_h^p(\phi_{y,k}) \,.$$

`mpp/src/lib4_fem/algebra/Vector.hpp`

# Parallel linear algebra

This is represented in parallel additively by $\underline{A}^{\mathcal{P}} = \left(\underline{A}^p\right)_{p\in\mathcal{P}}$ and $\underline{b}^{\mathcal{P}} = \left(\underline{b}^p\right)_{p\in\mathcal{P}}$ with

$$\underline{A}^p_{yz} = \left(a^p_h(\psi_{z,j}, \phi_{y,k})\right)_{j,k} \in \mathbb{R}^{N^p_y \times N^p_z}, \qquad \underline{b}^p_z = \left(\ell^p_h(\psi_{z,j})\right)_j \in \mathbb{R}^{N^p_z}$$

defining $\underline{A}^{\mathcal{P}} : \underline{V}^{\mathcal{P}} \longrightarrow (\underline{V}^{\mathcal{P}})'$ and $\underline{b}^{\mathcal{P}} \in (\underline{V}^{\mathcal{P}})'$.
Note that the inner products $\left(\underline{A}^{\mathcal{P}}\underline{u}^{\mathcal{P}}\right) \cdot \underline{v}^{\mathcal{P}}$ and $\underline{b}^{\mathcal{P}} \cdot \underline{v}^{\mathcal{P}}$ are well-defined for consistent vectors $\underline{u}^{\mathcal{P}}$ and $\underline{v}^{\mathcal{P}}$ independently of the additive decomposition and the parallel distribution of $\underline{A}^{\mathcal{P}}$ and $\underline{b}^{\mathcal{P}}$.
For iterative solvers, we construct preconditioners $\underline{B}^{\mathcal{P}} : (\underline{V}^{\mathcal{P}})' \longrightarrow \underline{V}^{\mathcal{P}}$ which map additive vectors to consistent vectors. Note that this requires communication for the construction and for the application of parallel preconditioners; e.g., for the construction of a Jacobi preconditioner the diagonal matrix entries $\underline{B}_{zz} = \left(\sum_{p\in\pi(z)} \underline{A}^p_{zz}\right)^{-1}$ are collected from the processor set $\pi(z)$, and for direct solvers all additive entries have to be collected.
This extends to multilevel preconditioning using $\underline{V}_0, \ldots, \underline{V}_L$ on a sequence of meshes by defining prolongation operators $\underline{I}^{\mathcal{P}}_l : \underline{V}^{\mathcal{P}}_{l-1} \longrightarrow \underline{V}^{\mathcal{P}}_l$ for consistent vectors and corresponding restriction operators $\underline{R}^{\mathcal{P}}_l : (\underline{V}^{\mathcal{P}}_{l+1})' \longrightarrow (\underline{V}^{\mathcal{P}}_l)$ for additive vectors; in M++ these operations are assembled depending on the discretization, e.g., the restriction is the transposed matrix in case of Lagrange elements and the $\mathrm{L}_2$ projection for discontinuous Petrov-Galerkin methods.

# Elliptic model equation: Darcy flow in porous media

Let $D \subset \mathbb{R}^d$ be a domain with boundary $\partial D = \Gamma_\mathrm{D} \cup \Gamma_\mathrm{N}$. For a given permeability tensor $\kappa\colon \bar{D} \longrightarrow \mathbb{R}^{d\times d}_{\mathrm{sym}}$ in the Darcy model, the flux $\mathbf{q} = -\kappa\nabla u$ is determined from the pressure head $u\colon \bar{D} \longrightarrow \mathbb{R}$ by the volume balance $\operatorname{div}\mathbf{q} = 0$ and the boundary conditions $u = u_\mathrm{D}$ on $\Gamma_\mathrm{D}$ and $-\mathbf{q}\cdot\mathbf{n} = g_\mathrm{N}$ on $\Gamma_\mathrm{N}$.
For this model we test different finite element approximations. In the first test this is approximated with Lagrange elements: find $u_h \in V_h^c(u_\mathrm{D})$ solving

$$\int_D \kappa\nabla u_h\cdot\nabla\phi_h\,\mathrm{d}x = \int_{\Gamma_\mathrm{N}} g_\mathrm{N}\phi_h\,\mathrm{d}a\,, \qquad \phi_h \in V_h^c(0)\,.$$

Therefore, we define the affine linear subspace

$$V_h^c(u_\mathrm{D}) = \left\{v_h \in V_h\colon v_h(z) = u_\mathrm{D}(z) \text{ for } z \in \mathcal{V}\cap\Gamma_\mathrm{D}\right\}$$

with respect to essential boundary conditions and the corresponding linear subspace $V_h^c(0)$ for the test functions.
The approximation $(\mathbf{q}_h, u_h) \in W_h(-g_\mathrm{N}) \times Q_{0,h}$ with mixed finite elements is given by the saddle point problem

$$\int_D \kappa^{-1}\mathbf{q}_h\cdot\boldsymbol{\psi}_h\,\mathrm{d}x - \int_D u_h\operatorname{div}\boldsymbol{\psi}_h\,\mathrm{d}x = -\int_{\Gamma_\mathrm{D}} u_\mathrm{D}\psi_h\cdot n\,\mathrm{d}a\,,$$

$$\int_D \operatorname{div}\mathbf{q}_h\phi_h\,\mathrm{d}x = 0\,, \qquad (\boldsymbol{\psi}_h, \phi_h) \in W_h(0)\times Q_{0,h}$$

# Elliptic model equation: Darcy flow in porous media

Here, the Neumann data are essential boundary conditions included in

$$W_h(-g_N) = \left\{ \mathbf{w}_h \in W_h : \int_F \mathbf{w}_h \cdot \mathbf{n} \, \mathrm{d}a = -\int_F g_N \, \mathrm{d}a \text{ for } F \in \mathcal{F}, \ z_F \in \Gamma_\mathrm{N} \right\}.$$

Introducing a Lagrange multiplier space $M_h = \prod_F \mathbb{P}_0(F)$ for the element boundary flux and the discontinuous space $W_\mathcal{K} = \prod_K W_K$, the mixed approximation can be computed by $(\mathbf{q}_h, u_h, \lambda_h) \in W_\mathcal{K} \times Q_{0,h} \times M_h(-u_\mathrm{D})$ solving the extended saddle point problem

$$\begin{aligned}
\int_K \kappa^{-1} \mathbf{q}_h \cdot \boldsymbol{\psi}_h \, \mathrm{d}x - \int_K u_h \operatorname{div} \boldsymbol{\psi}_h \, \mathrm{d}x &= \int_{\partial K} \lambda_h \boldsymbol{\psi}_K \cdot \mathbf{n} \, \mathrm{d}a \,, && \boldsymbol{\psi}_K \in W_K \,, \\
\int_K \operatorname{div} \mathbf{q}_h \, \mathrm{d}x &= 0 \,, && K \in \mathcal{K} \,, \\
\sum_K \int_{\partial K} \mathbf{q}_h \cdot \mathbf{n} \, \mu_h \, \mathrm{d}a &= -\int_{\Gamma_\mathrm{N}} g_\mathrm{N} \, \mu_h \, \mathrm{d}a \,, && \mu_h \in M_h(0)
\end{aligned}$$

with $M(-u_\mathrm{D}) = \left\{ \mu_h \in M_h : \int_F \mu_h \, \mathrm{d}a = -\int_F u_\mathrm{D} \, \mathrm{d}a, \ F \in \mathcal{F}, \ z_F \in \Gamma_\mathrm{D} \right\}$.
Now, essential Dirichlet boundary conditions are included in the Lagrange multiplier space. Static condensation allows to reduce the global problem to a symmetric positive definite system for the Lagrange multiplier.
Then, $(\mathbf{q}_h, u_h)$ can be reconstructed by a local post-processing step.

# Elliptic model equation: Darcy flow in porous media

The Darcy equation can also be approximated by the discontinuous Galerkin method with symmetric interior penalty parameter $\gamma_F = \mathcal{O}(k^2/h)$ depending on the polynomial degree $k$ and the mesh size $h$

$$
\begin{aligned}
a_h^{\mathsf{dG}}(u_h, \phi_h) = &\sum_{K \in \mathcal{K}} \int_K \kappa \nabla u_h \cdot \nabla \phi_h \,\mathrm{d}x + \sum_{F \in \mathcal{F}_h \setminus \Gamma_\mathrm{N}} \gamma_F \int_F [u_h]_F \cdot [\phi_h]_F \,\mathrm{d}a \\
&- \sum_{F \in \mathcal{F} \setminus \Gamma_\mathrm{N}} \int_F \Big( \{\kappa \nabla u_h\}_F \cdot [\phi_h]_F + [u_h]_F \cdot \{\kappa \nabla \phi_h\}_F \Big) \mathrm{d}a \,, \\
b_h^{\mathsf{dG}}(\phi_h) = &\int_{\Gamma_\mathrm{N}} g_\mathsf{N} \phi_h \,\mathrm{d}a + \sum_{F \in \mathcal{F} \cap \Gamma_\mathrm{D}} \gamma_F \int_F u_\mathsf{D} \phi_h \,\mathrm{d}a \\
&- \sum_{F \in \mathcal{F}_h \cap \Gamma_\mathrm{D}} \int_F u_\mathsf{D} \kappa \nabla \phi_h \cdot n \,\mathrm{d}a \,, \qquad u_h, \phi_h \in Q_{k,h}
\end{aligned}
$$

using the face average $\{\phi_h\}_F = \frac{1}{2}(\phi_h|_K + \phi_h|_{K'})$ and the jump term on interior faces $[\phi_h]_F = n_K \phi_K + n_{K'} \phi_{K'}$ for $F \in \mathcal{F}$ with $\mathcal{V}_F = \mathcal{V}_K \cap \mathcal{V}_{K'}$.

# Elliptic model equation: Darcy flow in porous media

Numerical results for the different discretizations are presented for a test configuration $D \subset (0,1)^2$ with homogeneous material $\kappa \equiv 1$ and 15 impermeable inclusions, cf. Fig. 1. Here, we impose Dirichlet boundary conditions $u_{\mathsf{D}}(x) = 0$ on the bottom for $x \in \Gamma_{\mathsf{D}} = [0,1] \times \{0\}$, Neumann boundary conditions $g_{\mathsf{N}}(x) = -1$ for $x \in (0,1) \times \{1\}$, and homogeneous Neumann boundary conditions on the remaining boundary. The convergence is tested by the evaluation of the goal functional

$$\mathcal{G}(\mathbf{q}) = \int_{\Gamma_{\mathcal{G}}} \mathbf{q} \cdot \mathbf{n} \, \mathrm{d}a$$

evaluating the outflow along the boundary part $\Gamma_{\mathcal{G}} = (0.25, 0.5) \times \{0\}$. The results in Tab. 1 indicate clearly, that the mixed formulation is more efficient than Lagrange elements or low-order discontinuous Galerkin elements.

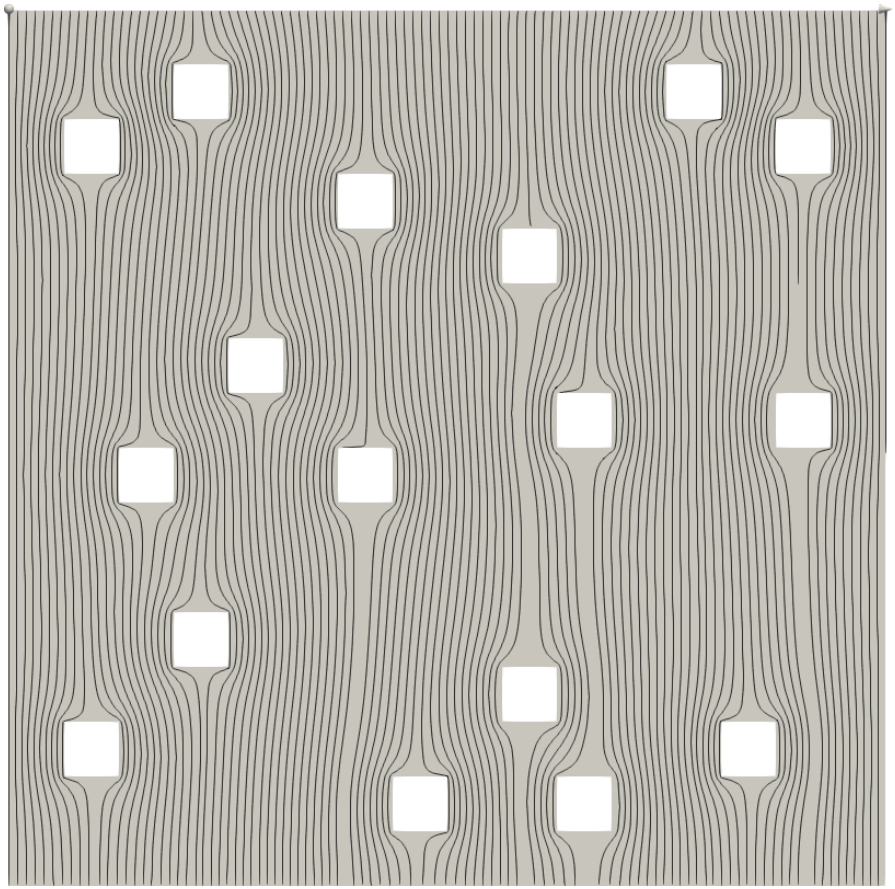

Figure: Streamline visualization of the flux $\mathbf{q}_h = \nabla u_h$ solving the Darcy equation with mixed finite element and mesh size $h = 2^{-10}$.

# Elliptic model equation: Darcy flow in porous media

| $\lvert\mathcal{K}\rvert$ | 478 | 1 912 | 7 648 | 30 592 | 122 368 | 489 472 | 1 957 888 |
|---|---|---|---|---|---|---|---|
| $\dim V_h^{\mathsf{c}}$ | 289 | 1 072 | 4 072 | 15 808 | 62 224 | 246 832 | 983 152 |
| $\mathcal{G}(\mathbf{q}_h)$ | 0.25660 | 0.25360 | 0.25239 | 0.25162 | 0.25117 | 0.25094 | 0.25082 |
| $\dim M_h$ | 783 | 3 000 | 11 736 | 46 416 | 184 608 | 736 320 | 2 941 056 |
| $\mathcal{G}(\mathbf{q}_h)$ | 0.24656 | 0.24940 | 0.25041 | 0.25062 | 0.25068 | 0.25069 | 0.25070 |
| $\dim Q_{1,h}$ | 14 34 | 5 736 | 22 944 | 91 776 | 367 104 | 1 468 416 | 5 873 664 |
| $\mathcal{G}(\mathbf{q}_h)$ | 0.25964 | 0.25428 | 0.25232 | 0.25151 | 0.25111 | 0.25090 | 0.25080 |
| $\dim Q_{2,h}$ | 2 868 | 11 472 | 45 888 | 183 552 | 734 208 | 2 936 832 | |
| $\mathcal{G}(\mathbf{q}_h)$ | 0.24776 | 0.25108 | 0.25080 | 0.25073 | 0.25071 | 0.25070 | |
| $\dim Q_{3,h}$ | 4 780 | 19 120 | 76 480 | 305 920 | 1 223 680 | 4 894 720 | |
| $\mathcal{G}(\mathbf{q}_h)$ | 0.25235 | 0.25066 | 0.25071 | 0.25071 | 0.25070 | 0.25070 | |
| $\dim M_{1,h}$ | 1 334 | 5 536 | 22 544 | 90 976 | 365 504 | 1 465 216 | |
| $\mathcal{G}(\mathbf{q}_h)$ | 0.25205 | 0.25096 | 0.25074 | 0.25071 | 0.25070 | 0.25070 | |

Table: Numerical approximation of the goal functional $\mathcal{G}$ for bilinear Lagrange elements, mixed elements in the hybrid formulation, discontinuous Galerkin elements for $k = 1, 2, 3$, and the weakly conforming method for $k = 2$.

# Hyperbolic model equation: linear transport

Depending on the Darcy flux $\mathbf{q}$, we consider a density $\rho\colon [0,T]\times\overline{D}\longrightarrow\mathbb{R}$ of some pollution which is transported by

$$\partial_t\rho+\operatorname{div}(\rho\mathbf{q})=0 \text{ in } (0,T)\times D\,,\qquad \rho(0)=\rho_0 \text{ in } D\,,$$

with inflow boundary condition

$$\rho=\rho_{\text{in}} \text{ on } (0,T)\times\Gamma_{\text{in}} \text{ with } \Gamma_{\text{in}}=\{x\in\partial D\colon \mathbf{q}\cdot\mathbf{n}<0\}\,.$$

Let $\Psi(\rho)=\rho q$ be the corresponding flux function, and let $\Psi^*$ be the numerical flux, defined by

$$\Psi^*_{K,F}(\rho_h)=\Psi(\rho_K) \text{ if } q\cdot n_K>0\,,\qquad \Psi^*_{K,F}(\rho_h)=\Psi(\rho_{K'}) \text{ if } q\cdot n_K<0$$

on inner faces $F=\partial K\cap\partial K'$, and $\Psi^*_{K,F}(\rho_h)=0$ for $F\subset\partial D\setminus\Gamma_{\text{in}}$.
We define the discrete operators $M_h, A_h$ and the right-hand side $b_h$ by

$$\begin{aligned}
(M_h\rho_h,\phi_h)_D &= (\rho_h,\phi_h)_D\,,\\
(A_h\rho_h,\phi_h)_D &= \Big(\sum_K -(\operatorname{div}\Psi(\rho_h),\phi_h)_K\\
&\qquad + \sum_{F\subset\partial K\setminus\Gamma_{\text{in}}}\big((\Psi(\rho_K)-\Psi^*_{K,F}(\rho_h))\cdot n_K,\phi_h\big)_F\Big)+(\Psi(\rho_h)\cdot n,\phi_h)_{\Gamma_{\text{in}}}\,,\\
(b_h,\phi_h)_D &= -(\Psi(\rho_{\text{in}})\cdot n,\phi_h)_{\Gamma_{\text{in}}}\,,\qquad \rho_h,\phi_h\in Q_h\,,
\end{aligned}$$

# Hyperbolic model equation: linear transport

The semidiscrete solution $\rho_h(t_{n+1}) = \exp(\triangle t\, M_h^{-1} A_h)\rho_h(t_n)$ in every time step $t_n = n\triangle t$ is approximated by the

- classical explicit Runge-Kutta method

$$\rho_h^{n+1} = \rho_h^n + \triangle t\, M_h^{-1} A_h \cdot \Big(\rho_h^n + \frac{1}{2}\triangle t\, M_h^{-1} A_h \big(\rho^n + \frac{1}{3}\triangle t\, M_h^{-1} A_h (\rho^n + \frac{1}{4}\triangle t\, M_h^{-1} A_h\, \rho_h^n)\big)\Big);$$

- implicit mid point rule

$$\rho_h^{n+1} = \rho_h^n + \triangle t \left(M_h - \frac{\triangle t}{2} A_h\right)^{-1} A_h\, \rho_h^n;$$

- polynomial Krylov method

$$\rho_h^{n+1} = V_m \exp(\triangle t\, H_m) V_m^\top M_h \rho_h^n$$

with $H_m = V_m^\top A_h V_m \in \mathbb{R}^{m\times m}$, $m \ll N$, where $V_m = [v_1, \ldots, v_m]$ is an $M_h$-orthogonal basis of the Krylov space

$$\operatorname{span}\left\{\rho_h^n, M_h^{-1} A_h \rho_h^n, \ldots, (M_h^{-1} A_h)^{m-1} \rho_h^n\right\},$$

i.e., $V_m M_h V_m^\top = I_m$.

# Hyperbolic model equation: linear transport

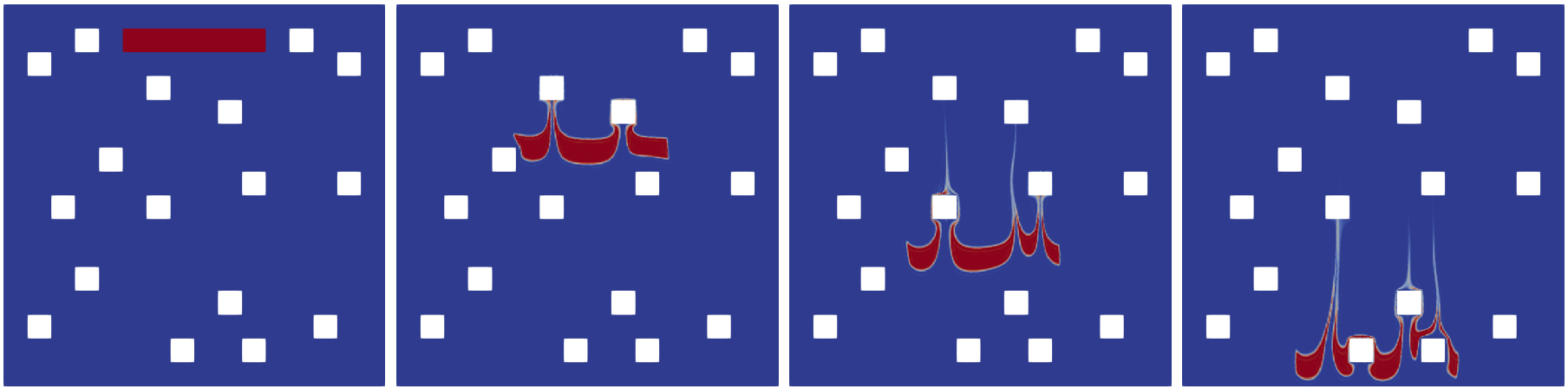

Figure: The transport of the initial distribution $\rho_0$ by the flow field $\mathbf{q}_h$ computed in Fig. 1 at $t = 0.25, 0.5, 0.75$ evaluated with the exponential time integrator, quadratic dG elements in space, and mesh size $h = 2^{-9}$.

| $\int_D \rho(1)\,\mathrm{d}x$ | $\triangle t = 0.004$ | | $\triangle t = 0.002$ | | $\triangle t = 0.001$ | | $\triangle t = 0.0005$ |
|---|---|---|---|---|---|---|---|
| $h = 2^{-7}$ | 1.79606 | | 1.83057 | | 1.83183 | | 1.83215 |
| | | 0.03451 | | 0.00126 | | 0.00032 | |
| $h = 2^{-8}$ | 1.60992 | | 1.63899 | | 1.64146 | | 1.64171 |
| | | 0.02907 | | 0.00247 | | 0.00025 | |
| $h = 2^{-9}$ | 1.61380 | | 1.63235 | | 1.63752 | | 1.63785 |
| | | 0.01855 | | 0.00517 | | 0.00033 | |

Table: Numerical approximation evaluated with quadratic discontinuous Galerkin elements.

# Parabolic equation: diffusion, convection, reaction

For the Darcy flux $\mathbf{q}$, a diffusion tensor $\kappa_c \colon \overline{D} \longrightarrow \mathbb{R}^{d\times d}$ and a nonlinear reaction rate $r \colon (0,T) \times D \times \mathbb{R} \longrightarrow \mathbb{R}$ we determine the concentration of a substance $c \colon [0,T] \times \overline{D} \longrightarrow \mathbb{R}$ by

$$\partial_t c - \operatorname{div}(\kappa_c \nabla c - c\mathbf{q}) = r(c) \;\text{ in }\; (0,T)\times D\,, \qquad c(0) = c_0 \;\text{ in }\; D$$

subject to the boundary conditions

$$\begin{aligned} c &= c_{\mathsf{D}} \text{ on } [0,T]\times\Gamma_{\mathsf{D}}\,,\\ \kappa_c\nabla c\cdot\mathbf{n} &= g_{\mathsf{N}} \text{ on } [0,T]\times\Gamma_{\mathsf{N}}\,,\\ \kappa_c\nabla c\cdot\mathbf{n} + \alpha c &= g_{\mathsf{R}} \text{ on } [0,T]\times\Gamma_{\mathsf{R}}\,. \end{aligned}$$

We define the bilinear form $a(\cdot,\cdot)$ and linear form $b(\cdot)$ by

$$\begin{aligned} a(c_h,\phi_h) &= \int_D \left(\kappa_c\nabla c_h\cdot\nabla\phi_h + q\cdot\nabla c_h\phi_h\right)\mathrm{d}x + \int_{\Gamma_{\mathsf{R}}} \alpha c_h\phi_h\,\mathrm{d}a\,,\\ b(\phi_h) &= \int_{\Gamma_{\mathsf{N}}} g_{\mathsf{N}}\phi_h\,\mathrm{d}a + \int_{\Gamma_{\mathsf{R}}} g_{\mathsf{R}}\phi_h\,\mathrm{d}a\,. \end{aligned}$$

Using an implicit Euler method, the approximation $c_h^n \in V_h(c_D(t_n))$ for step $n$ at time $t_n$ is determined by the nonlinear problem

$$\frac{1}{\triangle t}\left(c_h^n - c_h^{n-1},\phi_h\right)_D + a\left(c_h^n,\phi_h\right)_D = \left(r(c_h^n),\phi_h\right)_D + b(\phi_h)\,, \qquad \phi_h \in V_h(0)\,.$$

# Parabolic equation: diffusion, convection, reaction

For the stream-line diffusion method, we use with $\delta_K = \mathcal{O}(h)$

$$a_h^{\mathsf{sd}}(c_h, \phi_h) = a(c_h, \phi_h) + \sum_K \delta_K \int_K \Big( -\operatorname{div}(\kappa_c \nabla c_h) + q \cdot \nabla c_h - r'(\tilde{c}_h) c_h \Big) q \cdot \nabla \phi \, \mathrm{d}x \,,$$

$$b_h^{\mathsf{sd}}(\phi_h) = b(\phi_h) + \sum_K \delta_K \int_K f \, q \cdot \nabla \phi \, \mathrm{d}x$$

for the linearization at $\tilde{c}_h$, which yields for an appropriate choice of $\delta_K$ and $r' \leq 0$ a positive definite bilinear form also in case of small diffusion.

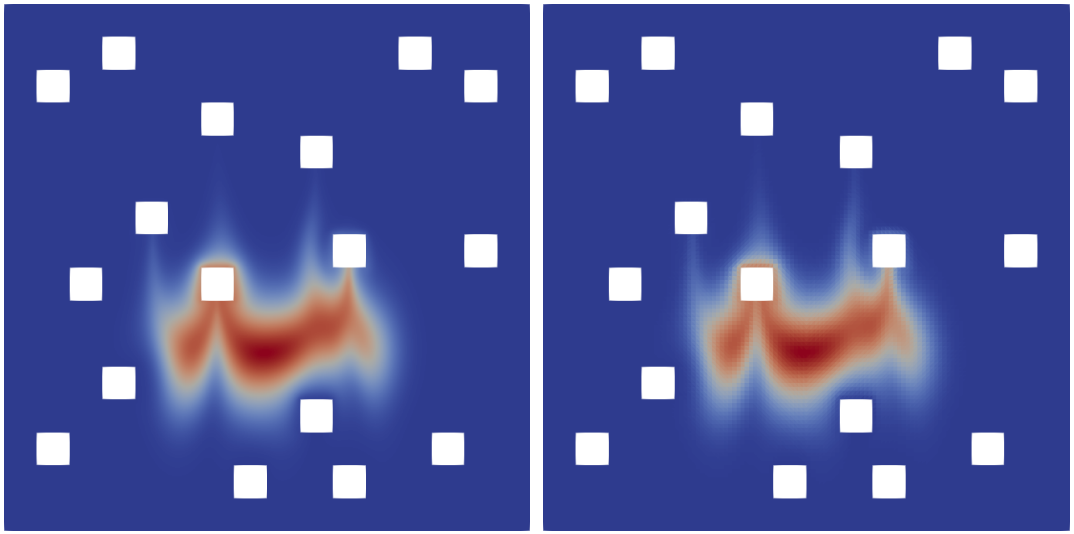

Figure: The diffusive and reactive transport of the initial distribution $c_0$ by the flow field $\mathbf{q}_h$ for the stream-line diffusion method.

# Gelfand problem

For $\lambda > 0$ we consider the nonlinear PDE $-\Delta u = \lambda \exp(u)$.

add `assemble/Gelfand.cpp` in `mpp/src/lib6_app/CMakeLists.txt`
add in `mpp/src/lib6_app/method/SingleExecution.cpp` the method Gelfand

create `conf/TUT_gelfand.conf`
create `conf/geo/Gelfand.geo`
create `mpp/src/lib6_app/pdesolvers/GelfandPDESolver.hpp`
create `mpp/lib6_app/assemble/Gelfand.hpp`
create `mpp/lib6_app/assemble/Gelfand.cpp`

```
mpirun -n 8 M++ TUT_gelfand initvalue_left=1 initvalue_right=1
mpirun -n 8 M++ TUT_gelfand initvalue_left=1 initvalue_right=4
mpirun -n 8 M++ TUT_gelfand initvalue_left=4 initvalue_right=1
mpirun -n 8 M++ TUT_gelfand initvalue_left=4 initvalue_right=4
paraview data/vtu/u.vtu
```

# Gelfand problem